NASA CR-134603

EFFECT OF PROOF TESTING ON THE FLAW GROWTH CHARACTERISTICS OF 304 STAINLESS STEEL

by
R. W. Finger

BOEING AEROSPACE COMPANY

Prepared
For

AEROSPACE SAFETY RESEARCH AND DATA INSTITUTE
LEWIS RESEARCH CENTER
NATIONAL AERONAUTICS AND SPACE ADMINISTRATION

Contract NAS 3 - 17762

Paul M. Ordin, PROJECT MANAGER

FOREWORD

This report describes an investigation of the effect of proof testing on the cyclic crack growth rates of 304 stainless steel weldments. The work was conducted at the Boeing Aerospace Company under NASA contract NASA 3-17762 from July 1973 to April 1974. The program was administered by Mr. Paul Ordin of the NASA Lewis Research Center.

Boeing people who participated in the program include J. N. Masters, Project Leader and R. W. Finger, Principal Investigator. Program support was supplied by A. A. Ottlyk, Test Support, C. W. Bosworth, welding, E. C. Robert, metallurgical investigation, and George Buehler, technical illustration.

The information contained in this report is also released as Boeing Document D180-18020-1.

TABLE OF CONTENTS

SYMBOLS

K_I	Opening Mode Stress Intensity Factor
a	Crack Depth of Semi-Elliptical Surface Flaw
a_i	Value of a at beginning of test
a_f	Value of a at termination of test
$2c$	Crack length at specimen face for semi-elliptical surface flaw
$2c_i$	Value of $2c$ at beginning of test
$2c_f$	Value of $2c$ at termination of test
σ	Uniform gross tensile stress acting perpendicular to plane of crack
σ_{ys}	Uniaxial tensile yield stress
ϕ	Complete elliptical integral of the second kind corresponding to the modulus $K = \left[(c^2 - a^2)/c^2\right]^{1/2}$
Q	$\phi^2 - 0.212\ (\sigma/\sigma_{ys})^2$
t	Gage area thickness of test specimen
R	Stress ratio, $\left(\text{minimum stress}/\text{maximum stress}\right)$
M_F	Scalar factor used to account for effect of stress free front plate surface on stress intensity factor for surface flaws.
M_K	Scalar factor depending on a/t and $a/2c$ used to account for effect of stress free back plate surface on stress intensity factor for surface flaws.
ΔK	Kmax - K min
$\frac{da}{dn}$	Cyclic crack growth rate $\left(\frac{\Delta a}{\Delta \text{ cycles}}\right)$

LIST OF TABLES

LIST OF ILLUSTRATIONS

SUMMARY

This experimental program was undertaken to determine the effect of proof test magnitude and frequency on the crack propagation rate of 304 stainless steel as-welded welds. General approach employed was testing of precracked surface flawed specimens under different loading spectrum.

All testing was accomplished using one weld metal surface flawed specimen configuration with approximately the same size initial defect introduced into the weld centerline from the weld root pass side. The cyclic stress level used was representative of the nominal membrane stress generally encountered in full scale vessels. Overload frequency effect tests were conducted at room temperature with an overload ratio of 1.5. Overload magnitude effect tests were conducted at overload ratios of 1.25, 1.50 and 1.75, together with an overload frequency of once every 1001 cycles. The overload was applied at room temperature and the cyclic loads were applied at 78K (-320F). All tests were terminated when the flaw penetrated the rear surface of the specimen.

Test results indicate that proper selection of proof test magnitude and frequency can result in decrease in crack growth rate for stress levels representative of the nominal membrane stress generally encountered in a full scale vessel.

1.0 INTRODUCTION

This investigation is the second of two experimental programs aimed at defining better guidelines for the proof testing of full scale 304 stainless steel over-the-road cryogenic vessels. The initial study investigated the fracture and sub-critical crack growth characteristics of 304 stainless steel weldments. Results of this study are presented in NASA CR-121025 entitled, "Fracture and Crack Growth Resistance Studies of Cryogenic Vessles." The original study concluded that it is unlikely that a fracture would originate at a crack like defect during the operation of an over-the-road transportable vessel fabracted from 304 stainless steel. It was observed, however, that very frequent proof testing could result in a reduction in cyclic life and therefore, recommended that more work be done to characterize the effects of proof test frequency and magnitude. This investigation was designed specifically to ascertain the effects of overload magnitude and frequency.

The experimental program conducted under the investigation consisted of cycling precracked 304 stainless steel surface flawed specimens until the flaw penetrated through the specimen thickness. All testing was conducted on weldments using stress levels representative of the nominal membrane stress encountered in full scale vessels designed to the stress values recommended by the ASME Boiler and Pressure Vessel Code, Section VIII, Division 1. The variables investigated were overload frequencies and overload magnitude. The overload frequency tests were conducted at room temperature using an overload ratio of 1.50. The overload magnitude tests used an overload frequency of 1000 cycles; here the overload was applied at room temperature and the cycles were applied at 78K (-320F).

2.0 BACKGROUND

A large body of experience hus established the su·face flaw as the best model of potential failure origins in pressure vessels. Modified linear elastic fracture mechanics, using the stress intensity factor, has proven a very useful tool in characterizing the subcritical crack growth and failure behavior of the surface flaw (1).* For the surface flaw the maximum stress intensity factor occurs at the maximum depth and is usually expressed by:

$$K_I = M_K M_F \sigma \sqrt{a\pi/Q}$$

M_F and M_K are parameters to account for the effects of both the front and rear su·face, a complete discussion of these parameters is supplied in Reference (2). The other parameters (a, Q) are explained in Figure 1. Available fracture theory works best when the critical flaw size, at stress levels below yield, is less than the material thickness. For these conditions it is possible to use a proof test to guarantee a residual cyclic life for a pressure vessel.

Presently, the Department of Transportation requires that all over-the-road cryogenic vessles be proof tested every two years. In order to gain some insight as to the effectivenss of this procedure, an experimental program was conducted; the results of which are published in NASA-CR-121025, "Fracture and Crack Growth Resistance Studies of 304 Stainless Steel Weldments Relating to Retesting of Cryogenic Vessels." This study concluded that it was unlikely that a catastrophic failure would initiate at a crack-like defect in an annealed 304 stainless steel vessel during its normal service life. A reduction in cyclic life was noted, however, for specimens subjected to a proof overload every 31 cycles. High stress levels typical of those that could be encountered around fittings welded into the vessel or in out-of-contour geometry areas were used in these tests;

* Numbers in parenthesis refer to references at end of report.

reported in the reference report. Because of this observation, it was recommended that additional work be conducted in order to characterize the effects of proof overload frequency and magnitude on cyclic crack propagation rate. This prog-gram was undertaken in order to accomplish this.

3.0 TEST PROGRAM

The test program undertaken to investigate the effects of proof overloads on the cyclic crack growth behavior of annealed 304 stainless steel weldments is summarized in Table 1. All testing was accomplished using surface flawed specimens having the flaws introduced into the weld centerline from the root pass side. The test program consisted of three primary tasks, one each for obtaining baseline data, the effect of overload frequency and the effect of overload magnitude. All of the tests were conducted at 1 Hz (60 cpm) using a sinusoidal loading profile and a minimum stress of approximately zero ($R \approx 0$). The peak cyclic stress level used 129.6 MN/m^2 (18.8 ksi) is representative of the nominal membrane stresses encountered in full scale vessels. Tests were terminated when the flaw had penetrated the rear surface of the specimen. The Task I tests were conducted at room temperature without any overloads in order to obtain baseline data to be used in the analysis of Task II and Task III results. In Task II, overload frequency effects, tests were conducted at room temperature with an overload ratio of 1.50. A total of four different overload frequencies were tested. Task III employed an overload period of 1001 cycles together with three different overload ratios in order to ascertain the effect of overload ratio. The overloads were applied at room temperature and the cycles were applied at 78K (-320F) in Task III.

4.0 MATERIALS AND PROCEDURES

4.1 Materials

The AISI 304 stainless steel plate material used in test specimen fabrication was originally purchased for NASA contract NAS 3-12003 (Fracture and Crack Growth Resistance Studies of 304 Stainless Steel Weldments Relating to Re-testing of Cryogenic Vessels). The plate material 0.95 by 122 by 244 cm (0.375 by 48 by 96 inch) was purchased in the annealed condition per MIL-S-5059C. The AISI 305 weld wire, both spooled 1.6 mm (1/16 inch) diameter and straight length 2.38 mm (3/32 inch) diameter used for welding were purchased per MIL-R-5031B, Class 1. Specification limits on chemical composition for both the plate material and weld wire are presented in Table 2.

The mechanical property data generated at the Boeing Company for the as-welded welds is presented in Table 3. The corresponding tensile data from NAS CR-121025 (Reference 3) is also presented in Table 3.

The average values obtained from the duplicate tests performed under each program are summarized below:

Test Temp. °K (°F)	Ultimate Strength MN/m^2 (ksi)	Yield Strength MN/m^2 (ksi)	Reduction in Area %	Elongation %	
295 (72)	607.5 (88.1)	308.6 (44.8)	55	55	
78 (-320)	1236.3 (179.3)	408.9 (59.3)	19	26	[1]
295 (72)	580.2 (84.2)	336.1 (48.8)	39	31	[2]
78 (-320)	829.1 (120.3)	398.9 (57.9)	14	14	[2]

[1] Subject Contract [2] Initial Study NASA CR-121025

The only mechanical properties which exhibited good agreement between the two studies were the yield strengths (both RT and 78 (-320)) and the room temperature ultimate strength. Presently, an explanation for the increased ductility and ultimate strength (at 78 (-320)) of the specimens tested in this study is not available.

4.2 Procedures

4.2.1 Welding

Weld panel halves 0.953 x 35.6 x 121.9 cm (0.375 x 14.0 x 48.0 inch) were machined with a 30° bevel and a 0.165 cm (0.065 inch) deep land as shown in Figure 2. The panel halves were set up using a 0.318 cm (0.125 inch) root gap and predistorted 0.318 cm (0.125 inch), as shown in Figure 2, to allow the halves to shrink into a flat panel at completion. Prior to welding, the edge preparations were wire brushed and cleaned with a methyl ethyl Ketone (MEK) solution. Welding was accomplished using a single manual GTA (Gas Tungsten Arc) root pass followed by two manual GMA (Gas Metal Arc) fill passes. "3M Brand" Stainless Steel Welding Backup Tape, Type SJ-8017X was used to support the GTA root pass weld, as shown in Figure 2. The initial GTA pass was deposited using a Vickers 300 ampere DC welding power source. Argon torch gas shielding, at 0.56 m^3/hr (20 CFH) was used in a Linde HW-18 torch. The manual GMA weld passes were applied using a Linde SVI-500, DCRP power source, a Linde ST-5 welding torch with torch shielding gas of 0.42 m^3/hr (15 CFH) argon. Between all passes the weld beads were wire brushed with a power driven stainless steel bristle brush. Welding parameters are listed below:

Pass No.	Location	Welding Process	Wire Type	Wire Dia. cm(in)	Current (amps)	Voltage Volts	Travel Speed cm/min (in/min)
1	Bottom	Manual GTA	AISI 308 Rod	0.24 (3/32)	150	15	7-10 (3-4)
2	Top	Manual GMA	AISI 308 Wire	0.16 (1/16)	280-300	29-32	25 (10)
3	Top	Manual GMA	AISI 308 Wire	0.16 (1/16)	280-300	29-32	25 (10)

After welding, all of the panels were X-rayed. The X-rays showed porosity in all of the panels. Areas of excessive porosity were denoted on the panels and were avoided during test specimen fabrication.

4.2.2 Specimen Preparation

All testing was accomplished with one mechanical property and one surface flawed specimen configuration; detailed specimen drawings are presented in Figure 3. All test specimens were drilled using existing drilling fixtures to ensure hole location within $\pm$ 0.025 mm (0.001 in.). The loading grips were drilled with the same fixtures to insure an accurate fit between test specimen and loading grips. For the surface flawed specimens, the area adjacent to the weld head was reduced in thickness. In general, a reduction in thickness to 0.900 cm (0.355 in.) was sufficient to clean up the weld bead. For the mechanical property specimens the entire specimen was reduced in thickness, in order to clean up the weld bead.

Starter slots were introduced into the surface flawed specimens by an Electric Discharge Machine (EDM). Circular electrodes along with a Kerosene dielectric were used. The electrodes were machined from 1.5 mm (0.06 in.) thick Packanite (a copper tungsten alloy). The electrode tips were machined with a 20° included angle terminating a circular section having a maximum radius

of 0.075 mm (0.003 inch). The starter slots were introduced into the weld centerline from the root pass side so that the flaw tip would end in an area of tensile residual stress. After EDM'ing, the starter slots were scrubbed clean using commercial grade naptha and a bristle brush, then blown dry with compressed air. After cleaning, the starter slots were covered with masking tape in order to protect them from contaminants. The starter slots were extended by means of low stress cyclic fatigue. The fatigue precracking was conducted in laboratory air using a maximum stress of 103 MN/m^2 (15 ksi) and a loading frequency of 10 Hz (600 CPM). In general, 10,000 to 20,000 cycles was sufficient to accomplish the fatigue precracking. A thirty power microscope was used to monitor the precracking procedure to ensure a precrack existed over the entire periphery of the starter slot.

4.2.3 Testing

Two different types of tests were conducted during the course of the program: mechanical property and cyclic crack growth.

Mechanical property tests were conducted both at room temperature in laboratory air and at 78K (-320F) in liquid nitrogen. In both cases a strain rate of 0.005 cm/cm/minute was used until the material yield strength was obtained; a strain rate of 0.02 cm/cm/minute was then used until failure occurred. Material properties obtained included ultimate strength, 0.2 percent offset yield strength, percent elongation in 5.08 cm (2.00 in.) gage length and percent reduction in area. These results are summarized in Table 3 and were discussed earlier in Section 4.1.

All of the cyclic crack growth tests were conducted on precracked surface flawed specimens on which pressure cups both front and rear were mounted for flaw breakthrough determination. One cup was left at ambient pressure and the other was pressurized with gaseous helium, to approximately 100 KN/m^2

(15 psi); when breakthrough occurred the ambient cup registered a pressure increase and the test was terminated. This procedure has been successfully employed on several previous research programs including that of Reference (3). A typical example of a test record obtained from this type of instrumentation is presented in Figure 4.

In addition to the pressure cups, all of the cyclic test specimens were equipped with crack opening displacement (COD) gages which provided a continuous record of crack opening displacement. The COD gages were attached to the crack surface as shown in Figure 5. A sinusoidal loading profile applied at 1 Hz (60 cpm) was used for the cyclic tests. Task I and Task II testing was conducted exclusively at room temperature, whereas, each Task III test was conducted partially at room temperature and partially at 78K (-320F). Task III tests consisted of repeatedly applying a loading block consisting of one room temperature overload followed by 1000 cycles at 78K (-320F). In order to expedite the warming up of the specimen, four heaters were employed. Figure 6 shows the manner in which the heaters, pressure cups, cryostate, etc. were applied to the specimen. Two thermocouples were used on each specimen to monitor the temperature. The application of loading cycles occurred only when specimens were within $\pm$ 5K ($\pm$9F) of their targeted value. A picture of the setup in operation is supplied in Figure 7.

5.0 RESULTS AND DISCUSSION

Test results for the individual tasks are discussed separately, followed by general comments pertinent to all of the results.

TASK I - Baseline Cyclic Tests

Two tests were conducted to obtain baseline cyclic crack growth data to be used in the analysis of Tasks II and III results. Results of these two tests are presented in Table 4 and Figure 8. Some test results from Reference (3) are also presented in Figure 8. If the beneficial effect of the initial overload is disregarded, then the reduction in cyclic stress between Reference (3) and this program caused a fourfold increase in cycles to breakthrough. If the following expression (from Reference (4))

$$da/dN = C\Delta K^n$$

is used to characterize cyclic crack propagation, then the fourfold increase corresponds to an n of 3.0. This is a typical value of n for steels. The curve drawn through the data points in Figure 8 is for a n of 3.0. The symbols used in this report are defined on Page vii

TASK II - Overload Frequency Effect

Results from the eight overload frequency effect tests are oresented in Table 4 and Figure 9. The function of this task was to letermine the frequency at which an overload of 50% would result in the greatest increase in cycles to breakthrough. It is well established that the application of an overload can result in retardation of the crack growth rate immediately after the overload. The extent and duration of the retardation is dependent upon the magnitude of the overload. Offsetting the beneficial retardation effects is the growth associated with the overload cycle; this growth can be as much as two orders of magnitude (100x) greater than the growth that would be predicted from

uniform cyclic load crack growth rate data generated at the overload stress level.[5] The magnitude of the crack growth encountered during the overload is partially dependent upon the frequency of the overload. Under this task, all factors except overload frequency were held constant; three sets of tests were conducted using an overload period of 30, 100 and 1000 cycles. In addition, one set of tests was conducted with a single initial overload. To better illustrate the effect of overload frequency on cycles to breakthrough, a plot of relative cyclic life versus overload frequency is presented in Figure 10. Relative cyclic life is the ratio of cycles to breakthrough for an overloaded specimen to cycles to breakthrough for a straight cyclic specimen having the same initial remaining ligament (specimen thickness minus initial flaw depth). For the two specimens which were subjected to a single initial overload, the overload frequency was considered to be the total number of cycles required to cause breakthrough. Since all of the parameters except the overload frequency were held constant, the plot of overload frequency versus relative cyclic life reflects only the effect of the overload frequency. To help define the shape of the overload frequency versus relative cyclic life curve, a point was calculated for an assumed overload period of 5000 cycles, in the following manner. First, the average growth rate per loading block (1 overload plus 1000 cycles) for specimens 4-1 and 4-2 was calculated and found to be 5.1×10^{-6} cm/cycle (2.0×10^{-6} in/cycle). It was then assumed the single overload tests experienced the same amount of crack growth during their initial 1001 cycles and the average growth rate was calculated for the remaining cycles and found to be 7.9×10^{-6} cm/cycle (3.1×10^{-6} in/cycle). For an overload period of 5000 cycles the first 1001 cycles will grow 0.0051 cm (0.0020 in.) and the next 4000 cycles will progress at a rate of 5.6×10^{-6} cm/cycle (2.2×10^{-6} in/cycle). The 5.6×10^{-6} cm/cycle (2.2×10^{-6} in/cycle) rate is derived by linearly extrapolating between the average growth rates. Using these values, a relative cyclic life of 1.63

was obtained for an overload frequency of once every 5000 cycles. From Figure 10 it is apparent that an overload frequency of once every 600 to 2500 cycles is optimum in terms of cyclic life for the stress levels, etc. tested. Also, for an overload period of 30 cycles the beneficial retardation gained from the overload was offset by the crack growth of the overload so the net result was no change in cyclic life. Thus, an overload frequency greater than once every 30 cycles would result in a reduction in cyclic life for these test parameters.

TASK III - Overload Ratio Effects

The test results from the overload ratio effect tests are presented in Table 5. For this series of tests the overloads were applied at room temperature and the cycles were applied at 78K (-320F). All of the tests were conducted with an overload period of 1000 cycles and a cyclic stress of 129.6 MN/m^2 (18.8 ksi). Three sets of tests were conducted, one each at an overload ratio of 1.25, 1.50 and 1.75. Because the specimens were tested in tandem (see Section 4.2.3) there was a slight variation in the stress levels. The actual stress levels varied between 124.8 MN/m^2 and 134.5 MN/m^2 [18.1 ksi and 19.5 ksi]. The average crack growth rates for these tests were adjusted to a stress level of 129.6 MN/m^2 by multiplying the actual growth rate by $(\frac{129.6\ MN/m^2}{\text{cyclic stress}})^3$ $[(\frac{18.8\ ksi}{\text{cyclic stress}})^3]$. Adjusting crack growth rates in this manner is a consequence of using

$$da/dN = c(\Delta K)^n$$

to characterize cyclic crack growth. [4] When the fracture surfaces of the specimens were reviewed through a 30 power microscope, the crack growth associated with each loading block was clearly visible. There was no significant variation in the band width over the entire growth region. The adjusted average crack growth rates are plotted against overload ratio in

Figure 11. A curve was posted through the data and extrapolated back to an overload ratio of 1.00 to obtain a baseline growth rate to be used in the determination of relative cyclic lives. The relative cyclic lives (Relative Cyclic Life = $\frac{\text{Overload Crack Growth Rate}}{\text{Baseline Crack Growth Rate}}$) were calculated and are plotted against overload ratio in Figure 11. The baseline crack growth rate obtained by extrapolating back to an overload ratio of 1.00 is greater than the room temperature baseline growth rate by approximately 60%. For the overload period tested, an overload ratio of 1.50 appears to be about optimum for reducing crack growth rate. The relative cyclic life at an overload ratio of 1.50 is approximately the same as the relative cyclic life for an overload frequency of once every 1000 cycles obtained in Task II. If the overload period employed in Task III was increased, the relative cyclic life for the overload ratio of 1.75 would probably be greater than for the 1.50 overload ratio. For a period of 1000 cycles, apparently the increased retardation from the higher overload is compensated for by the increased crack growth associated with it.

With the exception of one test (Specimen 5-3, Table 4), not yet reported, all of the test data fell within a scatter band of ± 20%. Since normal data scatter for cyclic crack growth testing is ± 100%, this level of reproducibility is excellent. The exception, Specimen 5-3, was tested at room temperature with an overload period of 30 cycles and an overload ratio of 1.50. The initial remaining ligament was 0.178 cm (0.070 inch), therefore, breakthrough should have occurred around 22,000 cycles. A total of 81,297 cycles, however, were required to cause breakthrough. In order to gain some insight into this result, a metallurgical investigation was conducted on Specimen 5-3 and a reference Specimen 1-4. The investigation revealed only two metallurgical differences between the two specimens. First, the microstructure of 1-4 consisted of a coarse grain pattern that intersected the fracture line as a more or less blocky structure (see Figure 12),

whereas, the microstructure of Specimen 5-3 consisted of fine, laminar, radiating grains. Second, a microhardness check starting 0.229 mm (0.009 inch) from the fracture surface and continuing inward at 0.102 mm (0.004 inch) invervals was conducted and the following values were obtained:

DISTANCE FROM Fracture Surface		ROCKWELL B HARDNESS VALUES	
mm	(in.)	Specimen 1-4	Specimen 5-3
0.229	(0.009)	96.0	91.5
0.330	(0.013)	95.0	91.0
0.432	(0.017)	94.0	91.0
0.533	(0.021)	95.0	87.5
0.635	(0.025)	95.0	88.0

The average R_B hardness values are 95.0 and 89.8 for Specimens 1-4 and 5-3, respectively. This variation corresponds to approximately a 85 MN/m^2 (12 ksi) variation in strength level. The lower strength and hardness, in combination with a finer structure, are the only aspects of 5-3 that differ from the reference Specimen 1-4. That these two factors would have such a tremendous effect on crack growth rate seems very unlikely. In addition, other specimens machined from the same weld panel as 5-3 (5-1, 5-4 and 5-5) rendered very reasonable results. Presently there is no explanation available for the decreased crack growth rate of Specimen 5-3.

Finally, one specimen (Specimen 1-1, Table 4) was tested at room temperature with an overload period of 2000 cycles, an overload stress of 310.3 MN/m^2 (45.0 ksi), a cyclic stress of 206.9 MN/m^2 (30.0 ksi) and an initial remaining ligament of 0.127 cm (0.050 inch). The higher stress levels employed in this test were the same as the stress levels used in the initial study, reference 3. A total of 6060 cycles were required to cause breakthrough.

Test results reported in Reference 3 indicate that if only a single initial overload had been applied, breakthrough would have occurred in approximately 4200 cycles. Thus, the periodic overload increased the cyclic life by approximately 45%. This test was conducted solely to determine if an overload period of 2000 cycles and an overload ratio of 1.50 might be detrimental to high stress areas in full scale vessels. At room temperature the previously stated overload frequency and ratio will increase full scale vessel life both in areas subjected to nominal and higher than nominal stresses.

6.0 CONCLUSIONS AND RECOMMENDATIONS

Several comments and conclusions pertinent to the proof testing of full scale vessels are presented in this section. It must be recognized that these conclusions are based on a limited number of tests conducted on one heat of material. While specific results could vary slightly for a different heat of the same material, the observed trends should still be valid. Other work presently in progress at the Boeing Company indicates that overload effects are highly dependent upon alloy; therefore, extension of these conclusions to a different alloy system is not recommended.

For the room temperature overload frequency effect tests, it can be concluded that for an overload ratio of 1.50 and a cyclic stress equivalent to the nominal membrane stress encountered in full scale vessel, a proof frequency in excess of once every 30 cycles will result in a reduction in cyclic life. Further, the cyclic life will increase as the frequency of proof testing diminishes, reaching an optimum at an overload period of approximately 1000 cycles. At the same temperature and overload ratio, a very significant reduction (approximately 60%) in cyclic life was obtained for an overload period of 30 when stress levels representative of those encountered in out-of-contour geometry areas in full scale vessels was employed. At the higher stress levels (σ_{cyclic} = 206.9 MN/m^2) (30.0 ksi) one additional data point obtained for an overload period of 2000 cycles showed an increase in cyclic life of approximately 45%. On the basis of these two tests it appears as if a proof test period of less than 400-500 cycles could result in a reduction in cyclic life. It is recognized that different vessels will have different service requirements; therefore, the loading cycles encountered in a year of service will vary from vessel to vessel. Since out-of-contour geometry areas can be anticipated in all vessels, any proof test

procedure that would result in a vessel being proof tested more frequently than once every 400-500 cycles should be avoided.

From the overload ratio effect tests conducted with an overload period of 1000 cycles and the overloads being applied at room temperature, while the cycles (129.6 MN/m^2, 18.8 ksi) were applied at 78K (-320F), it can be concluded that the optimum proof overload ratio in terms of crack growth rate is approximately 1.50.

LIST OF REFERENCES

1. C. F. Tiffany, "Fracture Control of Metallic Pressure Vessels", NASA Space Vehicle Design Criteria (Structures) NASA SP-8040, May 1970.

2. R. C. Shah and A. S. Kobayashi, "On the Surface Flaw Problem", the Surface Crack: Physical Problems and Computational Solutions, ASME Publication, October 1972.

3. L. R. Hall and R. W. Finger, "Fracture and Crack Growth Resistance Studies of 304 Stainless Steel Weldments Relating to Retesting of Cryogenic Vessels, NASA CR-121025, December 1972.

4. P. C. Paris and F. Erdogan, "A Critical Analysis of Crack Propagation Laws", Transactions of ASME, Series D (Journal of Basic Engineering), Vol. 85, No. 4. 1963.

5. "Fracture and Fatigue Crack Growth Behavior of Surface Flaws and Flaws Originating at Fastener Holes", Air Force Contract AF33651-71-C-1687 (in work) to be published as an Air Force Contract Report in 1974.

TABLE 1: TEST PROGRAM FOR 304 STAINLESS STEEL AS-WELDED WELDS

Task	Loading Program Type	Loading Program Details: Overload σ_2 MN/m^2 (KSI)	Overload Temp °K (°F)	Cycling MN/m^2 (KSI)	Cycling Temp. °K (°F)	N (Cycles)
I	A	--	--	129.6 (18.8)	295 (72)	--
II	B	194.4 (28.2)	295 (72)	129.6 (18.8)	295 (72)	--
	C	194.4 (28.2)	295 (72)	129.6 (18.8)	295 (72)	30
	C	194.4 (28.2)	295 (72)	129.6 (18.8)	295 (72)	100
	C	194.4 (28.2)	295 (72)	129.6 (18.8)	295 (72)	1000
III	C	162.0 (23.5)	295 (72)	129.6 (18.8)	78 (-320)	1000
	C	194.4 (28.2)	295 (72)	129.6 (18.8)	78 (-320)	1000
	C	226.8 (32.9)	295 (72)	129.6 (18.8)	78 (-320)	1000

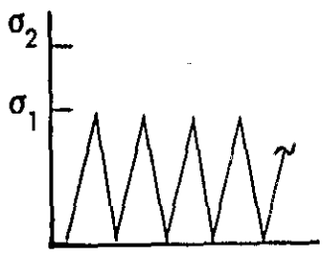

Loading Program A

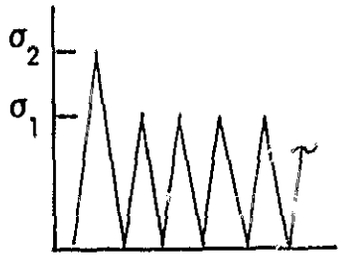

Loading Program B

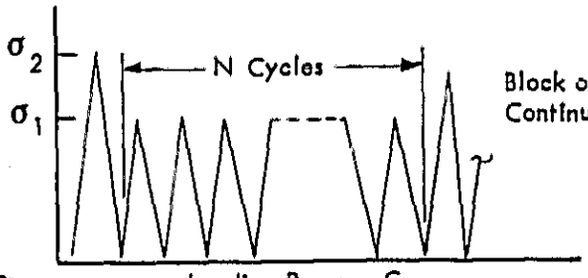

Loading Program C

TABLE 2: SPECIFICATION LIMITS ON CHEMICAL COMPOSITION FOR AISI 304 STAINLESS STEEL PLATE AND AISI 308 STAINLESS STEEL WELD WIRE

MATERIAL	LIMIT	ELEMENT (% BY WEIGHT)									
		Cr	Ni	C	Cu	Si	Mn	P	S	Mo	Fe
AISI 304 STAINLESS STEEL PLATE	MAX	20.0	12.0	0.08	0.50	1.00	2.00	0.045	0.030	0.50	Bal
	MIN	18.0	8.0	--	--	--	--	--	--	--	Bal
AISI 308 STAINLESS STEEL WELD WIRE	MAX	22.0	11.0	0.07	--	0.60	2.00	0.030	0.030	--	Bal
	MIN	20.0	9.5	--	--	0.25	1.0	--	--	--	Bal

TABLE 3: MECHANICAL PROPERTY TEST RESULTS FOR 304 STAINLESS STEEL WELDMENTS

Specimen Number	Gage Thickness cm (in)	Test Temperature °K (°F)	Ultimate Strength MN/m^2 (KSI)	2% Offset Yield Strength MN/m^2 (KSI)	Reduction in area %	% Elongation in 5.08 cm (2.0 in) Gage Length
T-1	0.871 (0.343)	295 (72)	601.2 (87.2)	310.3 (45.0)	53	49
T-2	0.899 (0.354)		613.7 (89.0)	306.8 (44.5)	57	61
		Average	607.5 (88.1)	308.6 (44.8)	55	55
T-3	0.897 (0.353)	78 (-320)	1130.1 (163.9)	388.2 (56.3)	14	24
T-4	0.869 (0.342)		1342.5 (194.7)	429.6 (62.3)	23	28
		Average	1236.3 (179.3)	408.9 (59.3)	19	26
SWT-1	0.897 (0.353)	295 (72)	577.1 (83.7)	318.5 (46.2)	42	31
SWT-2	0.909 (0.358)		583.3 (84.6)	353.7 (51.3)	36	31
		Average	580.2 (84.2)	336.1 (48.8)	39	31
SWT-3	0.645 (0.254)	78 (-320)	739.1 (107.2)	404.0 (58.6)	12	11
SWT-4	0.643 (0.253)		919.1 (133.3)	393.7 (57.1)	15	16
		Average	829.1 (120.3)	398.9 (57.9)	14	14

NOTE: Test results for specimens SWT-1, 2, 3, 4 from NASA CR-121025 (Reference 3).

TABLE 4: ROOM TEMPERATURE CYCLIC TEST RESULTS FOR 304 STALINESS STEEL WELDMENTS

Specimen Number	Gage Thickness † cm (in)	Initial Flaw Depth a_i	Initial Flaw Length $2C_i$ cm (in)	Initial Flaw Length $2C_f$ cm (in)	$t - a_i$ cm (in)	Loading Sequence	σ_1 MN/m^2 (KSI)	σ_2 MN/m^2 (KSI)	N	Cycles to Breakthrough	
4-4	0.899 (0.354)	0.696 (0.274)	4.37 (1.72)	4.42 (1.74)	0.203 (0.080)	A	129.6 (18.8)	--	--	18,795	
3-3	0.912 (0.359)	0.676 (0.266)	4.50 (1.77)	4.67 (1.84)	0.236 (0.093)	A	129.6 (18.8)	--	--	29,333	
4-3	0.894 (0.352)	0.678 (0.267)	4.47 (1.76)	4.60 (1.81)	0.216 (0.085)	B	129.6 (18.8)	194.4 (28.2)	--	26,197	
3-1	0.912 (0.359)	0.686 (0.270)	4.47 (1.76)	4.65 (1.83)	0.226 (0.089)	B	129.6 (18.8)	194.4 (28.2)	--	31,829	
4-1	0.899 (0.354)	0.701 (0.276)	4.52 (1.78)	4.60 (4.81)	0.198 (0.078)	C	129.6 (18.8)	194.4 (28.2)	1000	38,104	
4-2	0.919 (0.362)	0.660 (0.260)	4.50 (1.77)	4.78 (1.88)	0.259 (0.102)	C	129.6 (18.8)	194.4 (28.2)	1000	54,434	
5-1	0.927 (0.365)	0.706 (0.278)	4.52 (1.78)	4.62 (1.82)	0.221 (0.087)	C	129.6 (18.8)	194.4 (28.2)	100	29,504	
5-4	0.909 (0.358)	0.732 (0.283)	4.52 (1.78)	4.65 (1.83)	0.178 (0.070)	C	129.6 (18.8)	194.4 (28.2)	100	23,414	
1-4	0.904 (0.356)	0.726 (0.286)	4.55 (1.79)	4.65 (1.83)	0.178 (0.070)	C	129.6 (18.8)	194.4 (28.2)	30	19,630	
3-2	0.907 (0.357)	0.729 (0.287)	4.45 (1.75)	4.67 (1.84)	0.178 (0.070)	C	129.6 (18.8)	194.4 (28.2)	30	18,197	
5-3	0.909 (0.358)	0.706 (0.278)	4.57 (1.80)	4.98 (1.96)	0.203 (0.080)	C	129.6 (18.8)	194.4 (28.2)	30	81,297	[1]
1-1	0.876 (0.345)	0.749 (0.295)	4.42 (1.74)	4.47 (1.76)	0.127 (0.050)	C	205.9 (30.0)	310.3 (45.0)	2000	6,060	[1]

[1] See Pages 18, 19 for discussion of these Tests.

TABLE 5: CYCLIC TEST RESULTS FOR 304 STAINLESS STEEL WELDMENTS

Specimen Number	Gage Thickness t cm (in)	Initial Flaw Depth a_i cm (in)	Initial Flaw Length $2C_i$ cm (in)	Final Flaw Length $2C_f$ cm (in)	Stress σ_2 MN/m^2 (KSI)	Test Temp. During σ_2 °K (°F)	Stress MN/m^2 (KSI)	Test Temp. During σ_1 °K (°F)	t - a cm (in)	Cycles to Break-through
1-2	0.884 (0.348)	0.686 (0.271)	4.52 (1.78)	4.67 (1.84)	162.7 (23.6)	295 (72)	131.0 (19.0)	78 (-320)	0.196 (0.077)	17,018
2-1	0.907 (0.357)	0.742 (0.292)	4.55 (1.79)	4.85 (1.91)	158.6 (23.0)	295 (72)	127.6 (18.5)	78 (-320)	0.165 (0.065)	16,017
3-5	0.919 (0.362)	0.734 (0.289)	4.88 (1.92)	4.88 (1.92)	187.5 (27.2)	295 (72)	124.8 (18.1)	78 (-320)	0.185 (0.073)	22,023
3-4	0.851 (0.335)	0.711 (0.280)	4.62 (1.82)	4.80 (29.3)	202.0 (1.89)	295 (72)	134.5 (19.5)	78 (-320)	0.140 (0.055)	17,300
5-5	0.922 (0.363)	0.688 (0.271)	4.60 (1.81)	4.67 (1.84)	222.7 (32.3)	295 (72)	127.6 (18.5)	78 (-320)	0.234 (0.092)	29,500
2-8	0.889 (0.350)	0.711 (0.280)	4.60 (1.81)	4.60 (1.81)	231.0 (33.5)	295 (72)	132.4 (19.2)	78 (-320)	0.178 (0.070)	18,019

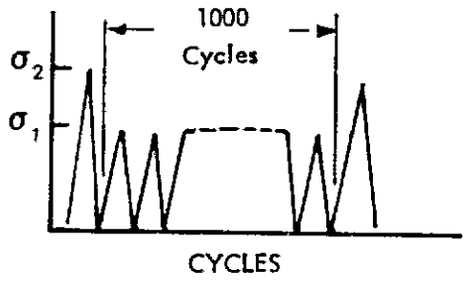

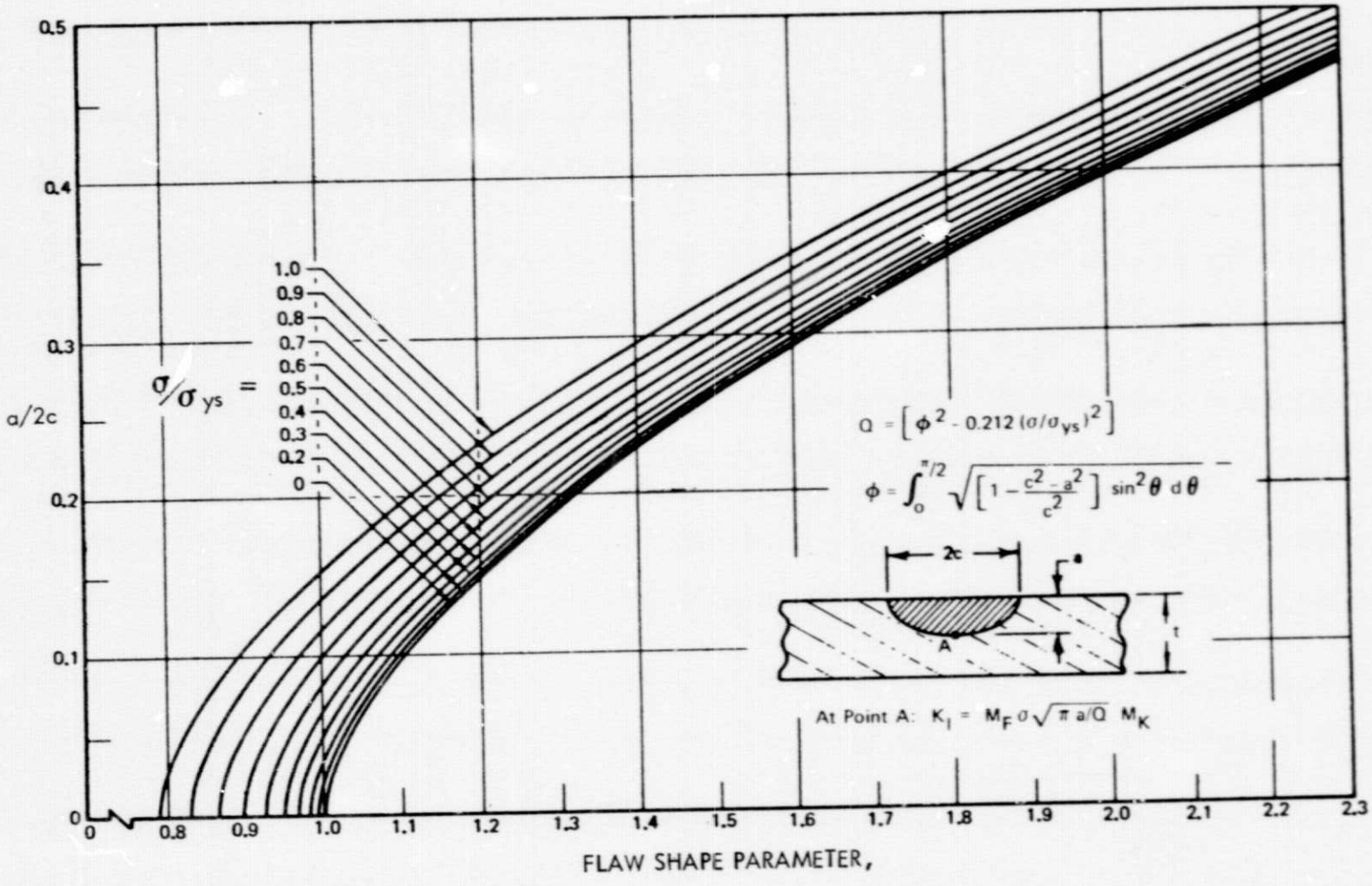

Figure 1: SHAPE PARAMETER CURVES FOR SURFACE FLAWS

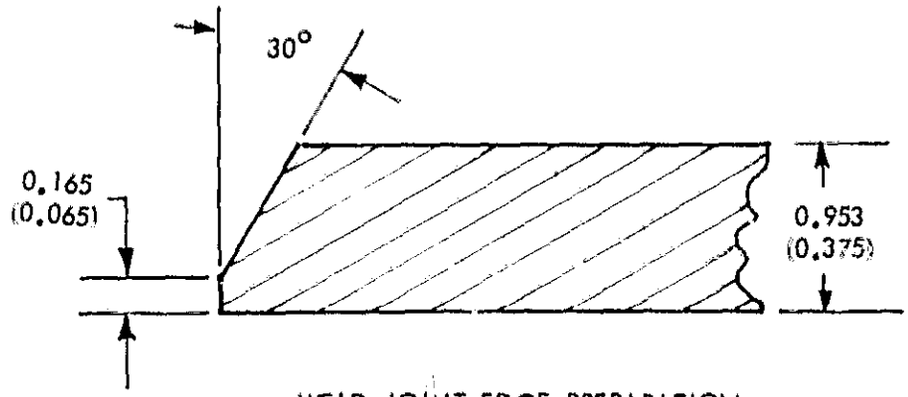

WELD JOINT EDGE PREPARATION

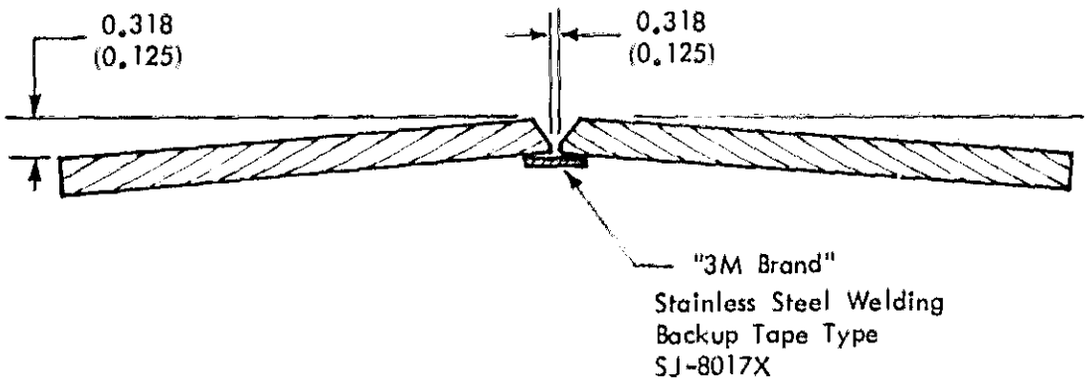

Dimensions Given in Centimeters (Inches)

Figure 2: WELD PANEL EDGE PREPARATION AND SETUP

Note: Dimensions Given in Centimeters (Inches)

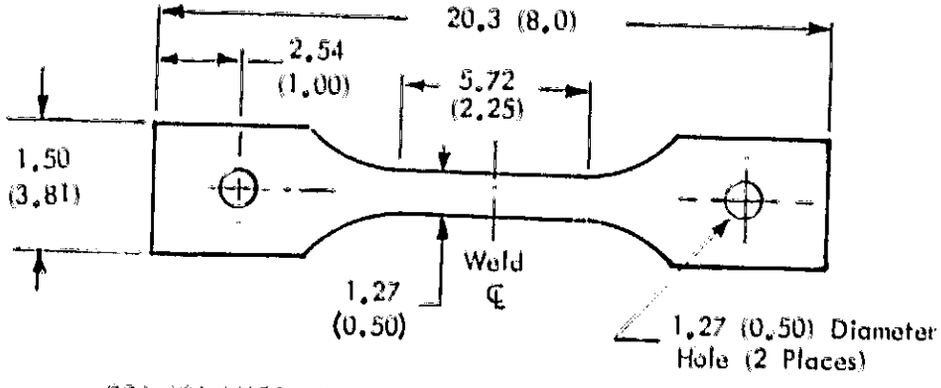

304 STAINLESS STEEL WELDMENT TENSILE SPECIMEN

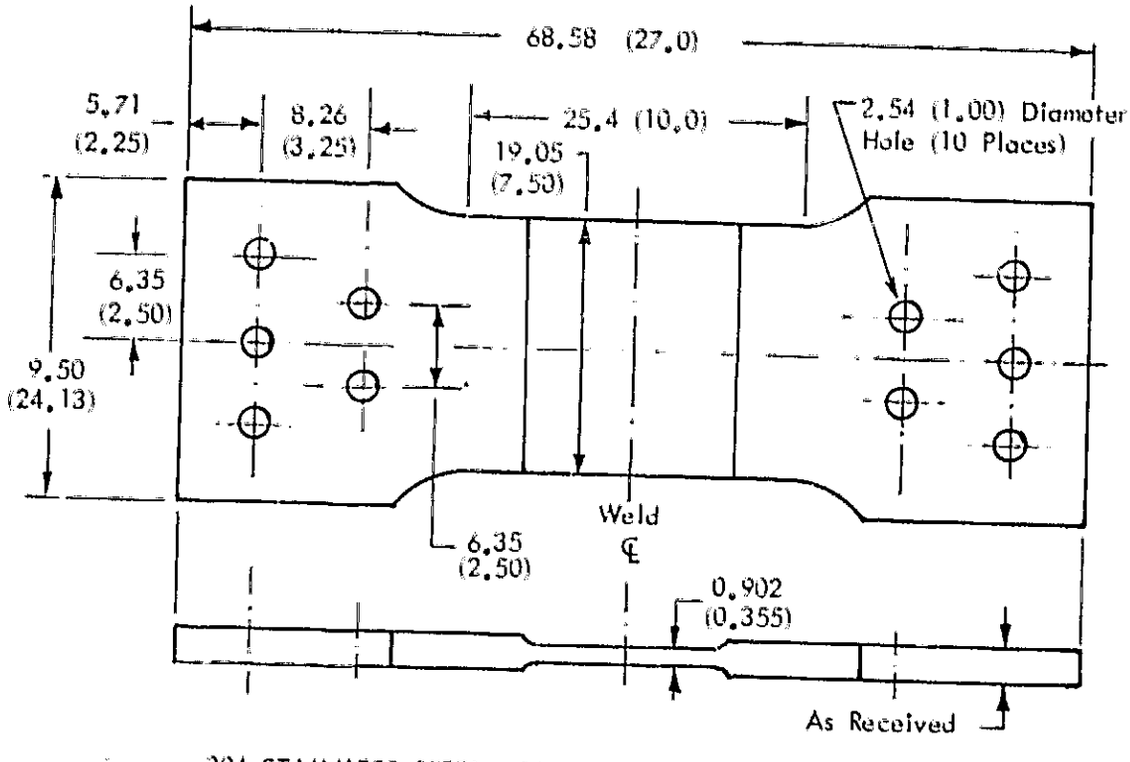

304 STAINLESS STEEL WELDMENT SURFACE FLAWED SPECIMEN

Figure 3: TEST SPECIMEN CONFIGURATIONS

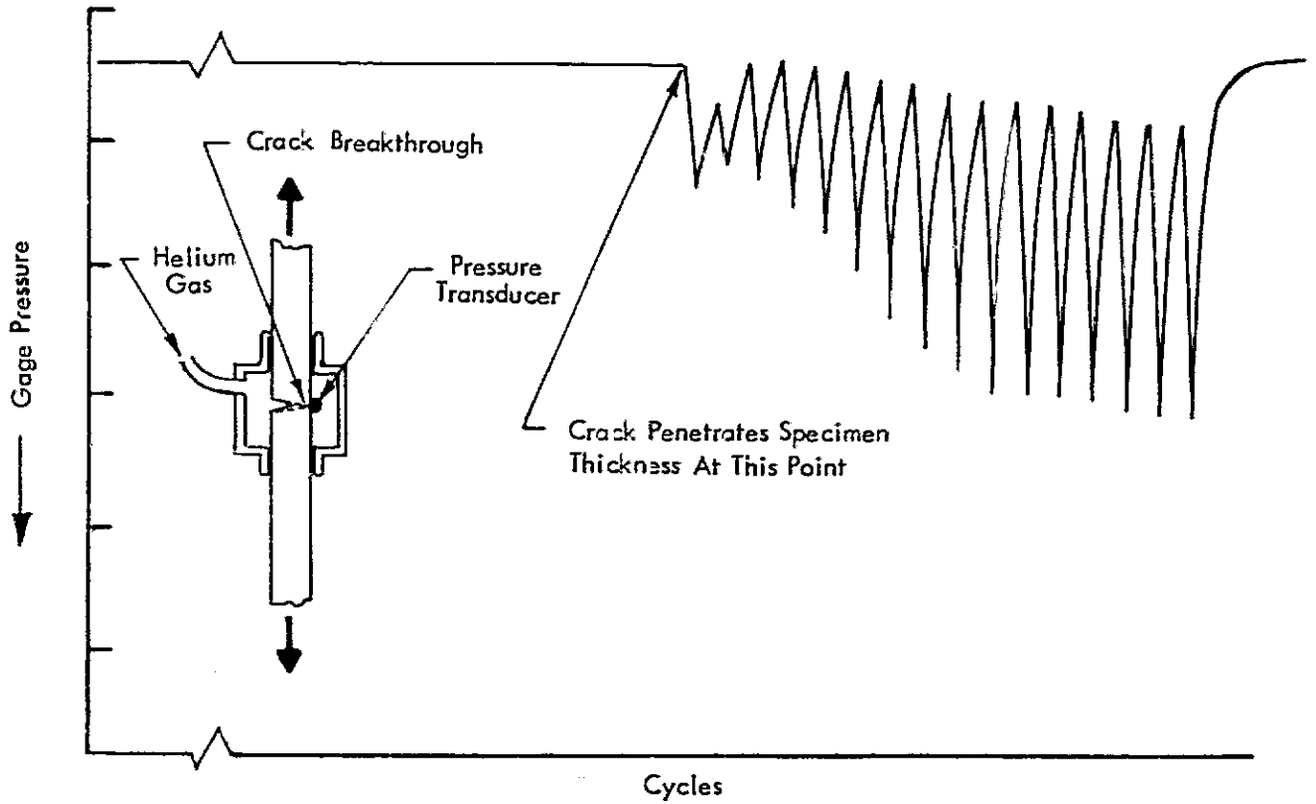

Figure 4: TYPICAL TEST RECORD OBTAINED FROM INSTRUMENTATION USED TO DETECT CRACK BREAKTHROUGH

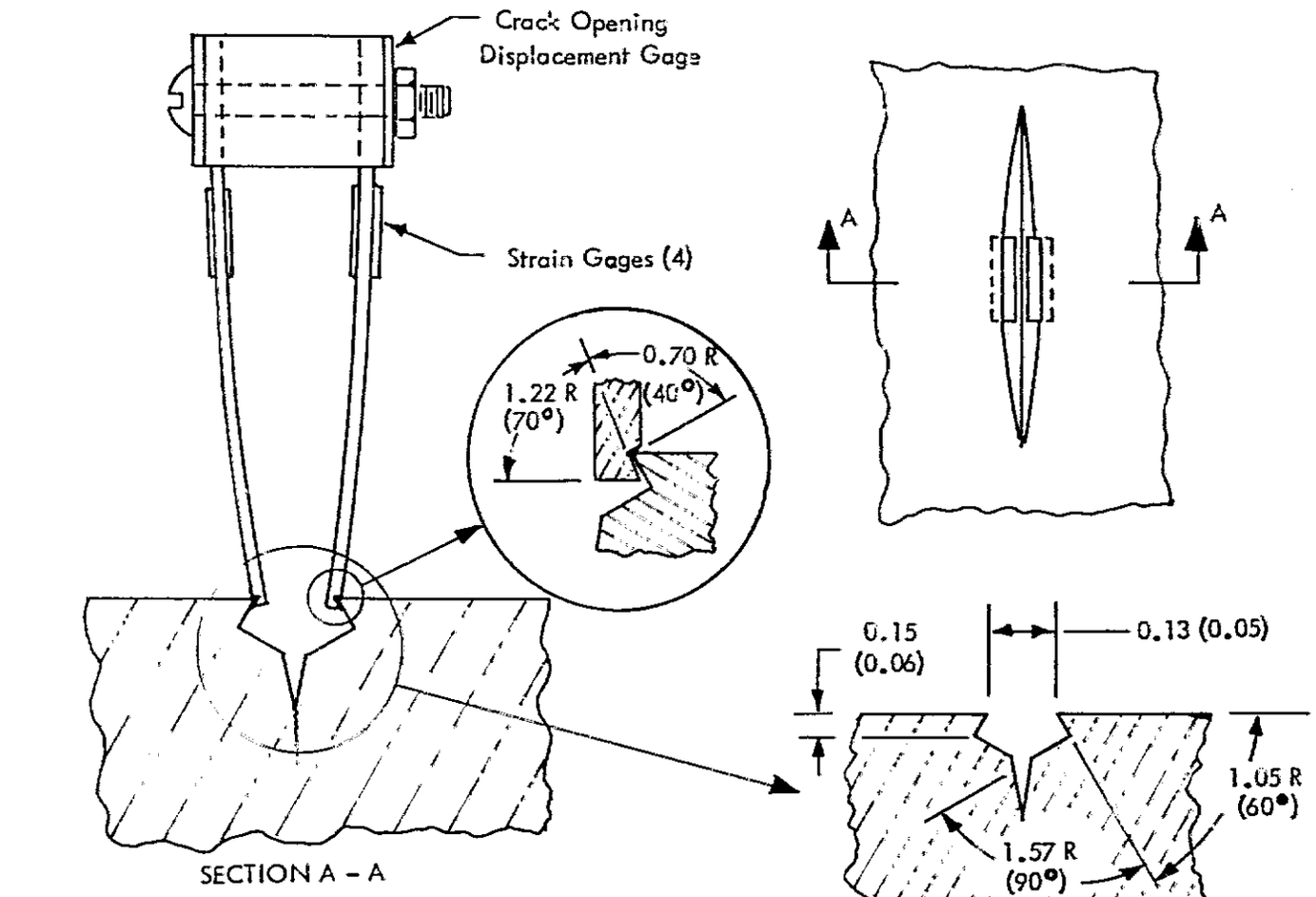

Figure 5: CLIP GAGE INSTRUMENTATION FOR CRACK OPENING DISPLACEMENT MEASUREMENTS

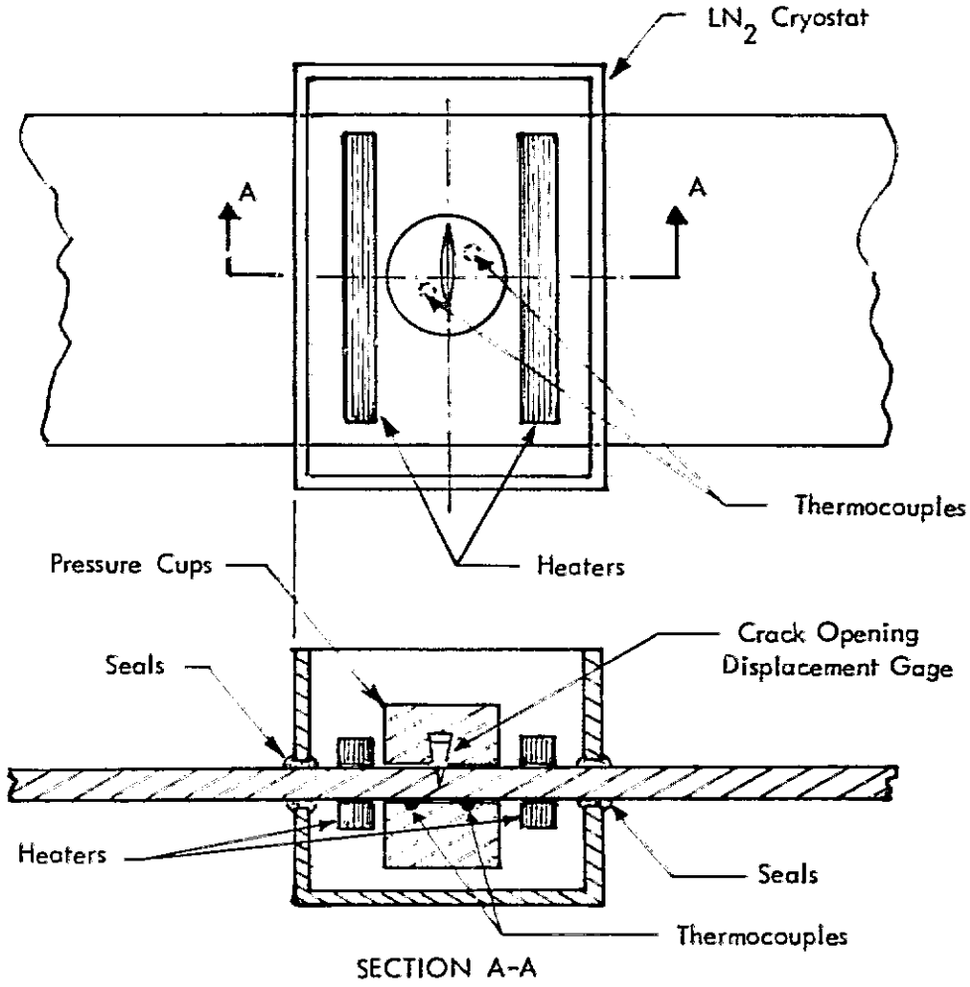

Figure 6: SPECIMEN INSTRUMENTATION FOR 304 STAINLESS STEEL SURFACE FLAWED SPECIMENS

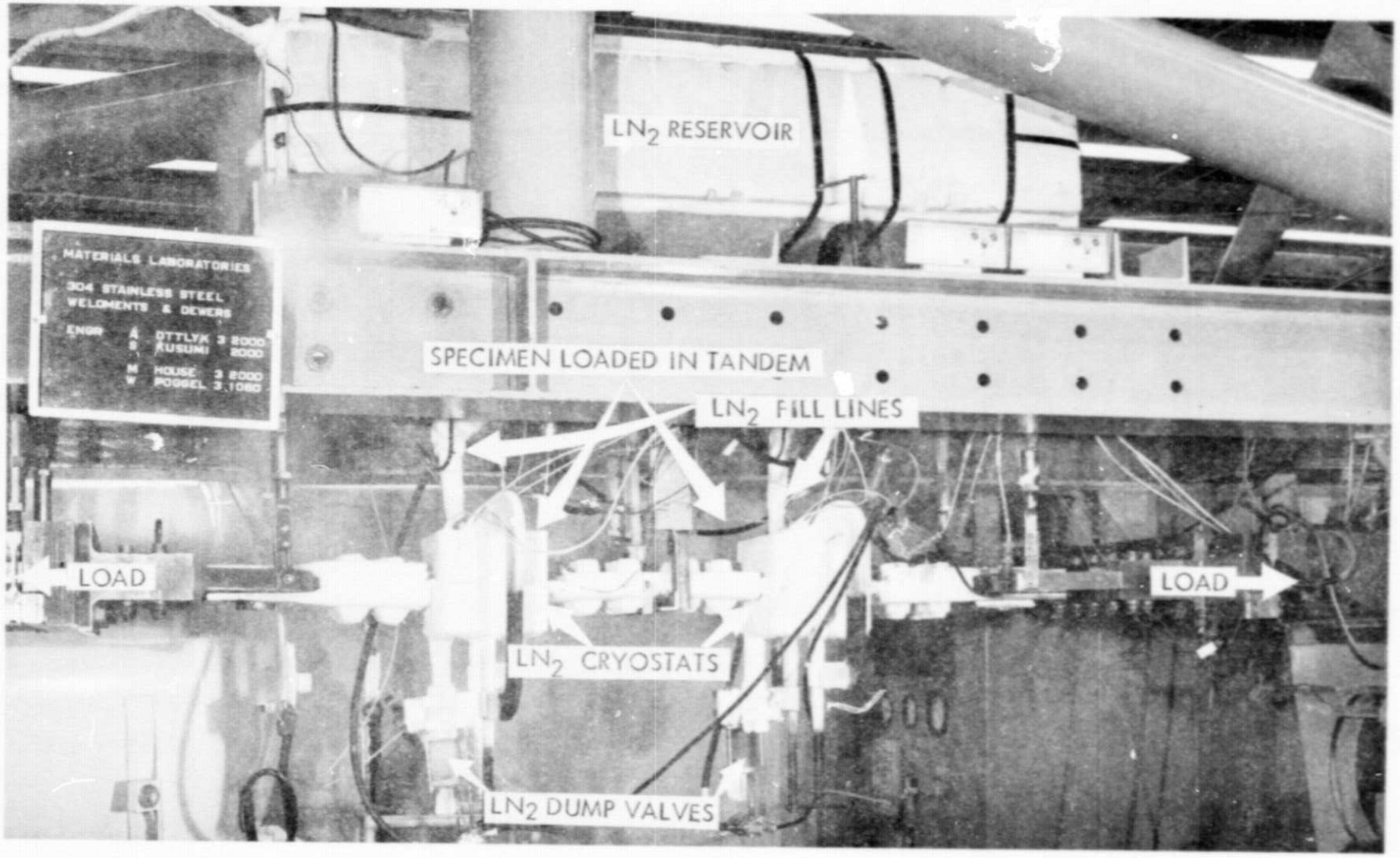

Figure 7: TEST SETUP

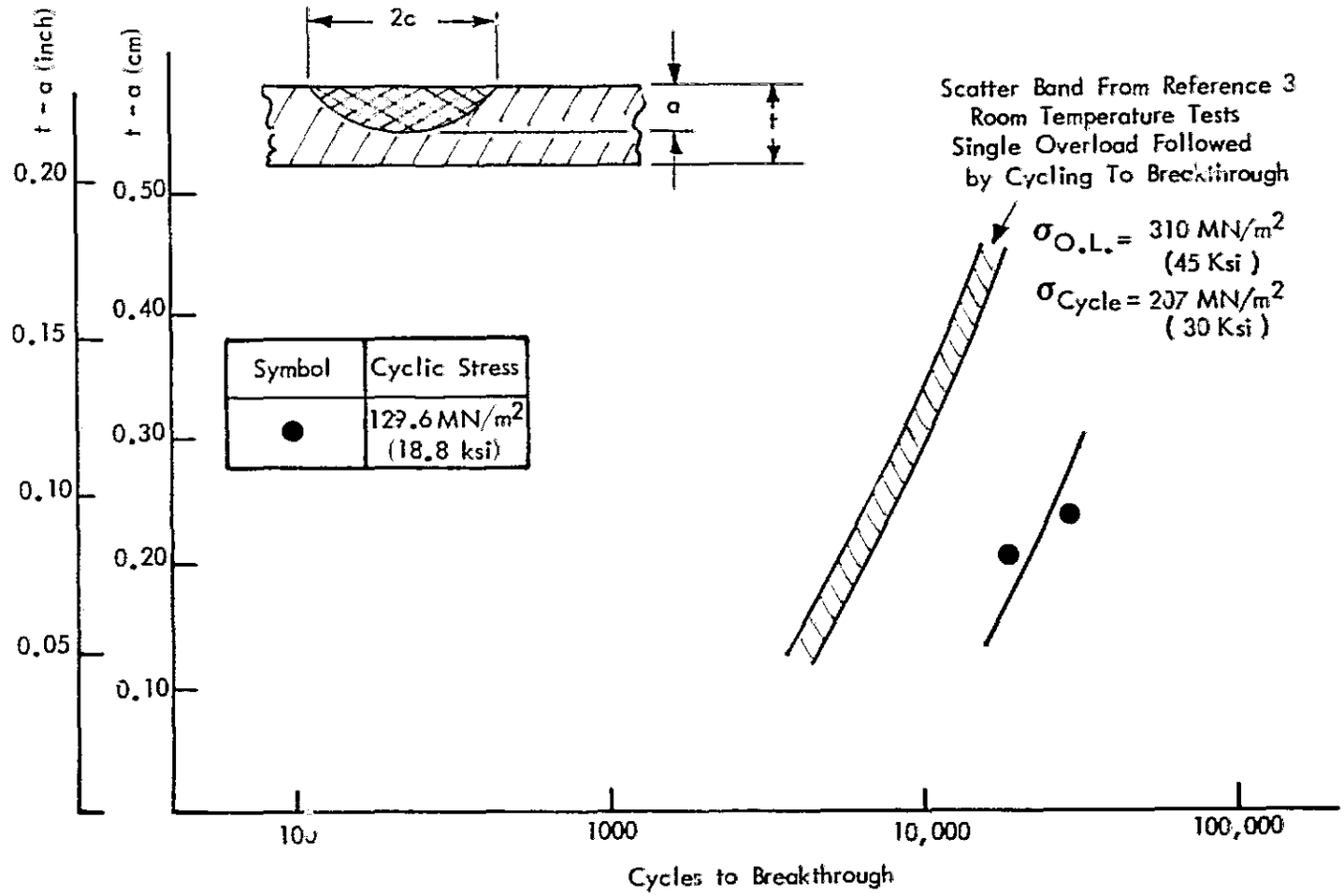

Figure 8: CYCLIC LOAD CRACK GROWTH RESULTS FOR 304 STAINLESS STEEL WELDMENTS

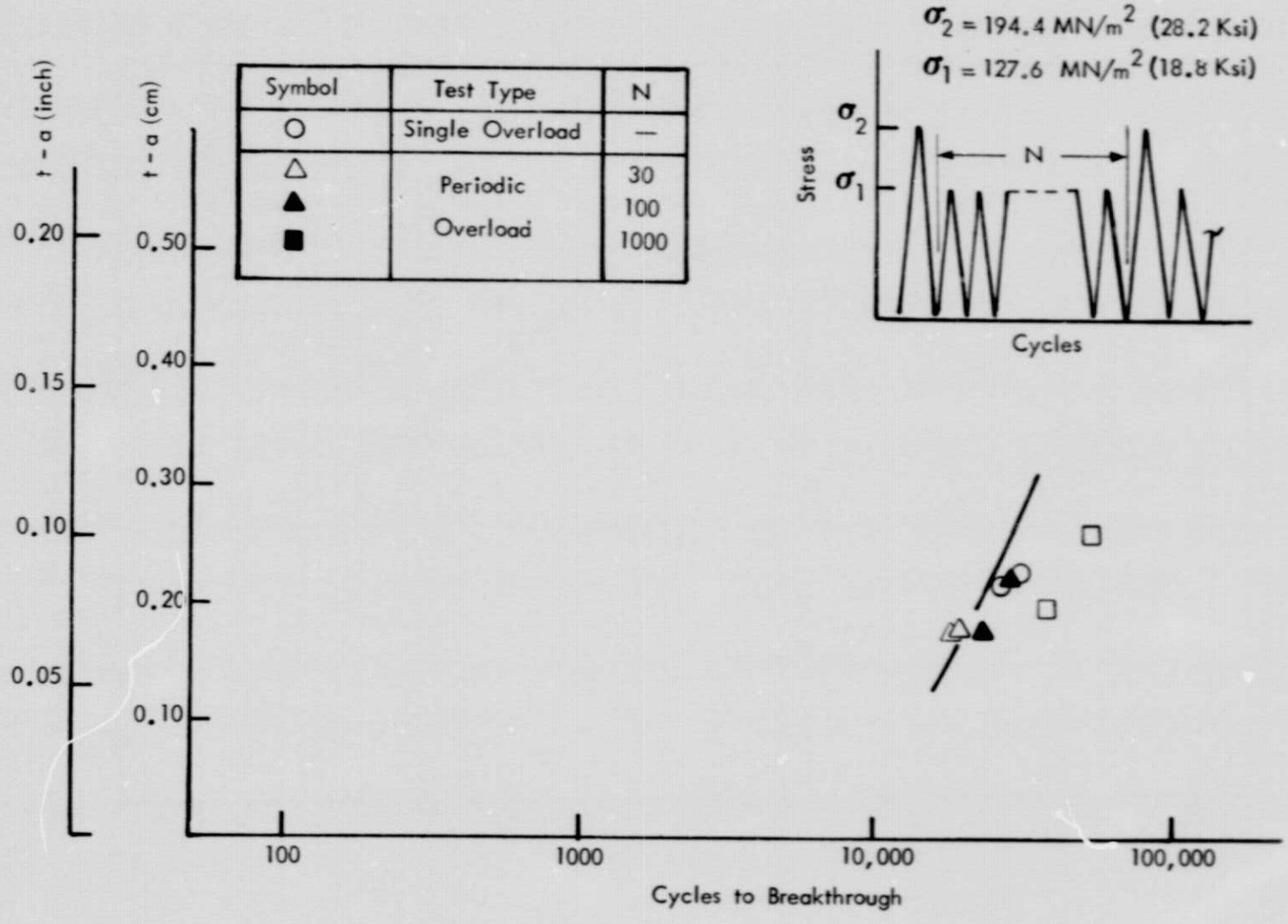

Figure 9: CYCLIC TEST RESULTS FOR PERIODICALLY PROOF TESTED 304 STAINLESS STEEL WELDMENTS

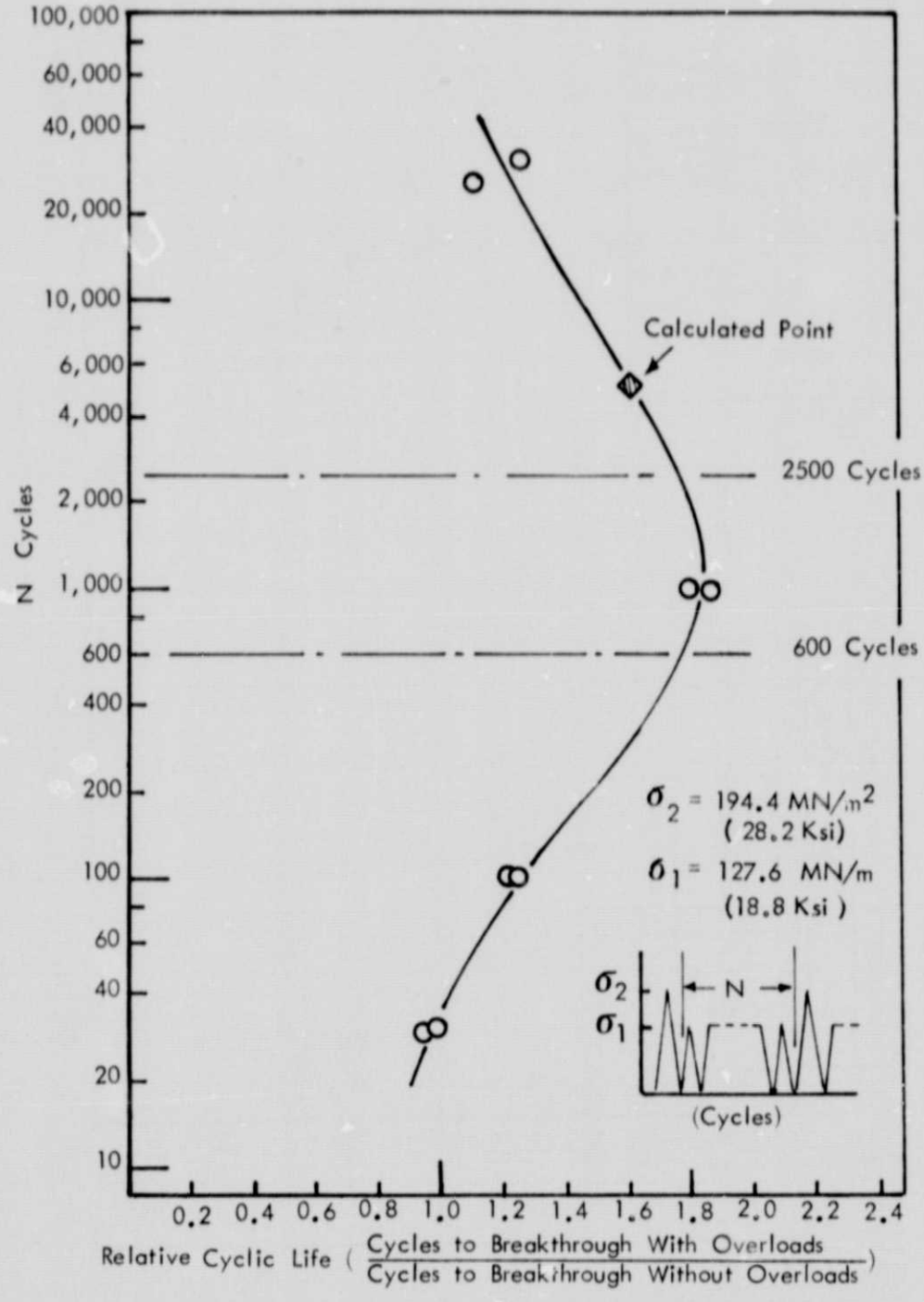

Figure 10: EFFECT IF OVERLOAD FREQUENCY ON RELATIVE CYCLIC LIFE

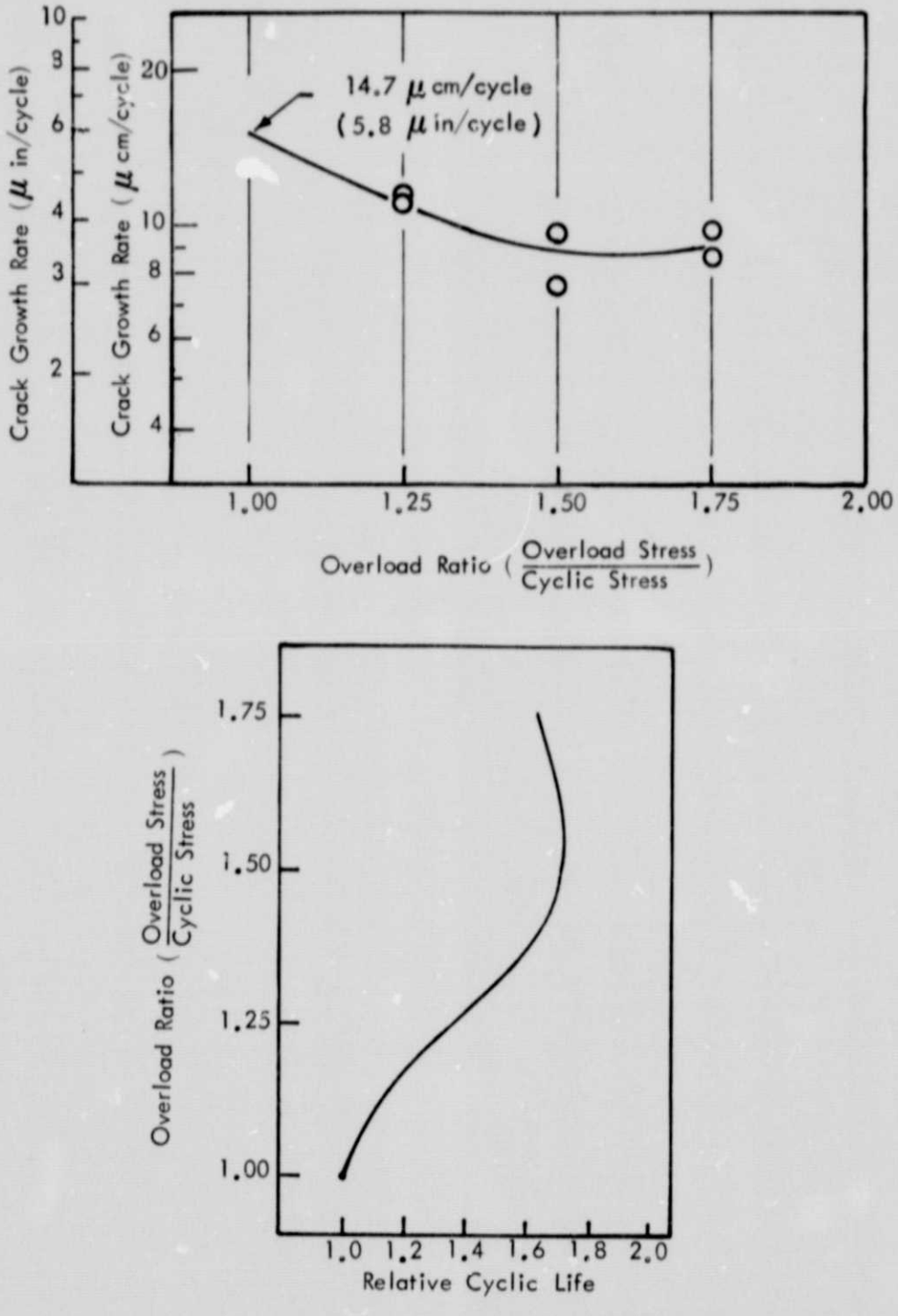

Figure 11: EFFECT OF OVERLOAD MAGNITUDE ON CYCLIC CRACK GROWTH RATES FOR 304 STAINLESS STEEL WELDMENTS

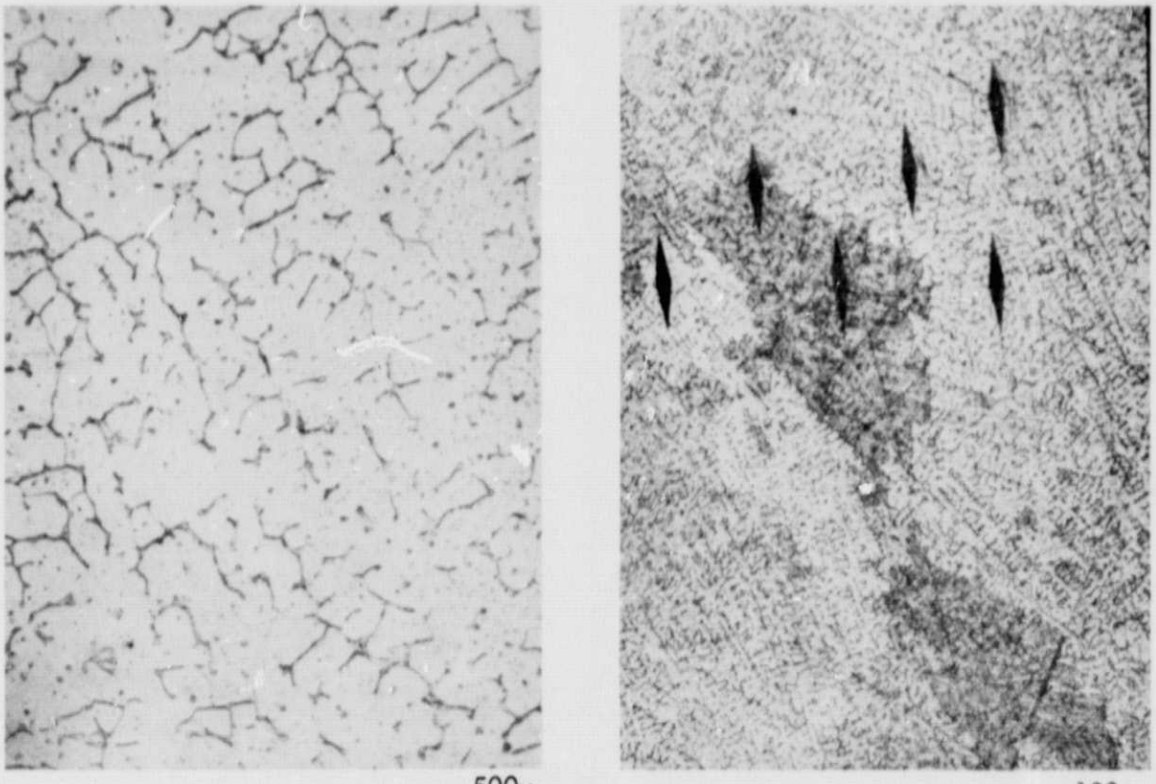

500x 100x

Specimen 1 - 4

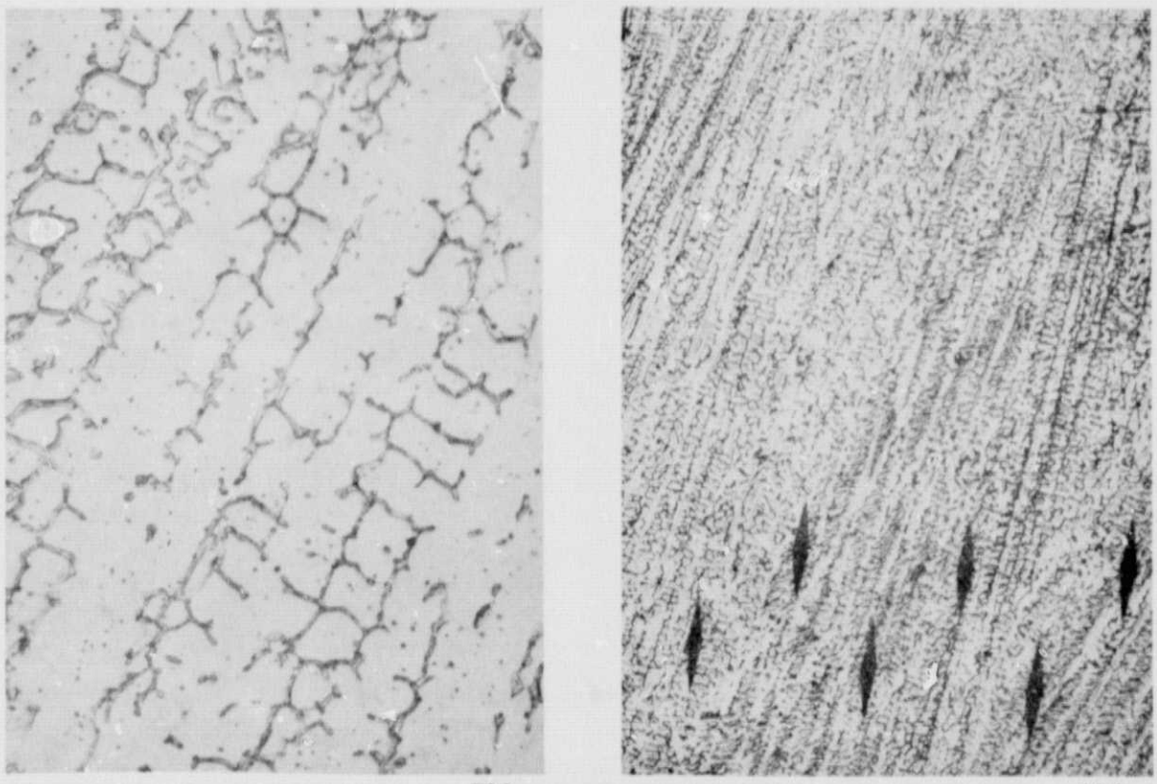

500x 100x

Specimen 5-3

Figure 12: MICROSTRUCTURE OF SPECIMENS 1-4 and 5-3